UDC 615.454
DOI: 10.15587/2519-4852.2026.358977

STUDY OF THE EFFECT OF THE MICROSTRUCTURE OF COMBINED AGGREGATES OF NONIONIC SURFACTANT AND CETOSTEARYL ALCOHOL ON THE RHEOLOGICAL PROPERTIES OF HYDROPHILIC CREAM BASES AND THE RELEASE OF ACTIVE SUBSTANCES IN EXPERIMENTS I*N VITRO*

Nikolay Lyapunov, Olena Bezugla, Oleksii Liapunov, Anna Liapunova, Igor Zinchenko, Yurij Stolper

The aim. *To study the effect of the microstructure of mixed aggregates and adsorption layers of non-ionic surfactant and cetostearyl alcohol (CSA) on the rheological characteristics of hydrophilic cream bases and the release of certain active substances in experiments in vitro.*

Materials and methods. *Cream bases with a dispersion medium of water and propylene glycol (9:1) were studied. The ratio of surfactant to CSA was varied within the base formulations. The rheological properties of the bases were analysed using rotational viscometry, and the microstructure of the aggregates was examined by the spin probe method employing four probes based on fatty acids. The release of active substances from the bases and solutions was tested in vitro; the content of active substances in the dialysate was determined by liquid chromatography.*

Results*. The apparent viscosity of the bases was observed to reach its maximum at certain ratios of surfactant to CSA, when coagulation structures were formed. The structural arrangement of mixed aggregates of surfactant and CSA was dependent on their ratio. It was demonstrated that a higher specific fraction of CSA in aggregates/adsorption layers contributed to lateral phase separation at the interface with the dispersion medium. This process led to the formation of solid CSA domains and liquid surfactant domains. The mixed aggregates of surfactant and CSA possessed a non-spherical configuration. The hydration of aggregates was ensured by non-ionic surfactant domains. These factors contributed to the formation of coagulation structures at certain concentrations of surfactant and CSA. An increase in the specific fraction of surfactant led to a tendency towards a homogeneous distribution of surfactant and CSA in their aggregates. This was accompanied by a decrease in the apparent viscosity of dispersed systems and a transition from creams to liquids. A decrease in the surfactant fraction resulted in a decline in the hydration of aggregates/adsorption layers, consequently leading to a decrease in the apparent viscosity of the bases. The release of ofloxacin or dexpanthenol was significantly retarded from the bases where coagulation structures were formed.*

Conclusions*. The rheological characteristics of hydrophilic cream bases are contingent on the microstructure of mixed aggregates or adsorption layers formed by nonionic surfactant and CSA. These properties can be modified by adjusting the mass ratios between these emulsifiers. In the case of cream bases, where a coagulation structure has formed, the release of active ingredients is found to be significantly retarded.*

Keywords*: cream base, apparent viscosity, aggregate, adsorption layer, surfactant, cetostearyl alcohol, spin probe, EPR spectrum, release*

How to cite:
Lyapunov, N., Bezugla, O., Liapunov, O., Liapunova, A., Zinchenko, I., Stolper, Yu. (2026). Study of the effect of the microstructure of combined aggregates of nonionic surfactant and cetostearyl alcohol on the rheological properties of hydrophilic cream bases and the release of active substances in experiments in vitro. ScienceRise: Pharmaceutical Science, 2 (60), 45–59. http://doi.org/10.15587/2519-4852.2026.358977

1. Introduction

Creams are semi-solid preparations of homogenous appearance, typically consisting of a lipophilic phase and an aqueous phase, one of which is finely dispersed in the other. In hydrophilic creams, the continuous phase is the aqueous phase. They usually contain oil-in-water emulsifiers combined, if necessary, with water-in-oil emulsifiers [1, 2]. Hydrophilic creams are o/w emulsions, but a dispersed system containing aggregates of o/w and w/o emulsifiers without an oil phase can be considered a cream.

In pharmacy, oil-in-water emulsions are widely used as bases for medicinal products containing hydrophilic and/or lipophilic active substances [3]. Emulsions are thermodynamically unstable systems; therefore, their physical stabilisation is an important issue in the pharmaceutical development of hydrophilic creams [4]. For this purpose, a variety of emulsifiers (both o/w and w/o) [5], surfactants [6], hydrophilic homopolymers [7], cellulose nanocrystals [8], aluminium oxide nanoparticles in combination with cationic surfactants [9], etc., are used. In the review [10], the prediction of the physical stability of semi-solid preparations, which are o/w emulsions, is discussed. It is important to note that the physical stability of emulsions is contingent upon the volume ratio of phases, the type and concentration of emulsifiers, the

hydrophilic-lipophilic balance (HLB) of emulsifiers, and the parameters of the technological process. It is emphasised that when developing the composition of emulsions, it is very important to possess a detailed understanding of the microstructure of adsorption layers and critical factors affecting the stability of emulsions [10].

Research into surfactants (emulsifiers) and emulsions has a long history [11–13], but many problems remain unresolved [6]. It is imperative to establish a correlation between the microscopic characteristics of the adsorption layer and the physical stability of emulsions on a macroscopic scale. It is imperative to ascertain the correlation between the rheological properties of emulsions and the structure of adsorption layers, as this will facilitate the control of the physicochemical properties of emulsions [14].

Hydrophilic surfactants, together with lipophilic surfactants, contribute to the formation of small, uniform droplets of the dispersed phase in oil-in-water emulsions, even with a high oil phase content [15]. The structure formed at the oil-water interface prevents the coalescence of oil-phase droplets [16]. In order to stabilise emulsions, the swift formation of viscoelastic interfaces between the aqueous and oil phases is necessary; these interfaces should consist of two types of surfactants (hydrophilic and lipophilic). It is necessary to understand the cooperative adsorption of these surfactants and the properties of the adsorption layers. A knowledge-based approach to emulsion development will replace empirical approaches [17]. A comprehensive understanding of the cooperative adsorption of these surfactants and the properties of the adsorption layers is imperative. A knowledge-based approach to emulsion development is set to supersede empirical methods [17]. The presence of mixed surfactants has been shown to result in a substantial reduction in interfacial tension between oil and water [18]. Understanding the effect of surfactant structure on the properties of the phase boundary surface and dynamic processes in emulsions is crucial for the rational development of stable emulsion compositions [18]. Currently, there is still limited understanding of the effect of different combinations of emulsifiers on the formation and stability of emulsions. This is a crucial aspect that should be given greater attention in future research. For instance, the HLB-based approach to emulsifier selection does not always provide a reliable prediction of the effectiveness of individual or mixed surfactants in emulsions [19]. Nevertheless, this approach remains in use for the development of stable o/w emulsions and the study of their properties [20–22].

One of the main issues in this field is the lack of analytical methods that can provide comprehensive insights into the composition and structural configuration of emulsifiers within extremely thin interfacial layers in real time [19].

In the study of the gel formed by cationic surfactant cetyl trimethyl ammonium chloride, cetearyl alcohol and water, rheological methods, small-angle X-ray scattering (SAXS) and diffusion NMR were utilised [23]. It was demonstrated that the gels possessed a locally lamellar structure, exhibiting periodic repeating distances of 31.4 nm and 28.5 nm in the cases of rapid and slow cooling, respectively. The cross-polarized microscopy images reveal the presence of multilamellar vesicles. The data on the supramolecular aggregates allowed rationalizing the mechanical behavior of these two samples of gel.

The complex of cetyl alcohol, cetomacrogol-1000 and water (1:1:1) was characterized by freeze-drying scanning electron microscopy, small-angle X-ray diffraction (SAXD), and ultra-SAXD etc. [24].

From our perspective, the spin probe method is the most informative for the study of micelles of surfactants and aggregates of surfactant with w/o emulsifiers [25, 26]. It has been demonstrated that, based on the EPR spectra of probe 4 palmitamido-2,2,6,6-tetramethylpiperidine-1-oxyl, the micelle cores are two-dimensional liquid in consistency and anisotropic in viscosity at 25°C. In the case of aggregates of nonionic surfactant and long-chain fatty alcohols C_{16}–C_{21} in an aqueous medium, lateral phase separation occurred with the formation of solid-like domains of long-chain fatty alcohols and liquid domains of nonionic surfactant. The hypothesis that mixed aggregates of surfactant and higher fatty alcohols possess a non-spherical configuration was debatable due to the limited research conducted with specific spin probes [27]. The study focused on a dispersion system with only a single mass ratio of nonionic surfactant to aliphatic alcohols. This limitation precluded the correlation of the composition of emulsifiers and the structure of their mixed aggregates with the rheological properties of the dispersion systems [27].

It should be noted that dispersed systems containing non-ionic, anionic, or cationic surfactants together with cetyl and stearyl alcohols are widely used in pharmaceutical formulations, particularly in the composition of creams. Examples of such products include Bepanthen® Plus cream (GP Grenzach Productions GmbH, Germany) [28] and Trimistyn®-Darnitsa ointment (Darnitsa Pharmaceutical Company, Ukraine) [29]. Certain emulsifiers are produced as a mixture of a surfactant and cetostearyl alcohol, for instance, Kolliphor CSL (BASF) [30].

The aim. To study the effect of the microstructure of mixed aggregates and adsorption layers of non-ionic surfactant and cetostearyl alcohol (CSA) on the rheological characteristics of hydrophilic cream bases and the release of certain active substances in experiments *in vitro.*

2. Planning (methodology) of the research

The experiment was planned incorporating a non-ionic surfactant, namely cetostearyl ether macrogol 20 (M20CSE), along with CSA. These excipients exhibit substantial disparities in their physicochemical properties [1, 30]. The objects of study comprised cream bases without an oil phase, which were dispersions of surfactant and CSA in a mixed solvent *water – propylene glycol* (PG) (90 : 10% w/w), in which the structure of water prevailed [31], as well as cream bases with an oil phase (o/w emulsions) and with the same emulsifiers and dispersion medium.

The study was planned to explore the rheological properties of cream bases using rotational viscometry, as

a function of the mass ratio of surfactant to CSA, with a constant dispersion medium composition and a temperature of 25°C.

The methodology encompassed the utilisation of the spin probe method to determine alterations in supramolecular configurations formed by surfactant and CSA molecules in a dispersion medium (in the absence and presence of an oil phase), which are concomitant with changes in the rheological characteristics of cream bases. Four spin probes, based on fatty acids, were used to detect surfactant and CSA aggregates at the boundary zone between polar and non-polar regions, as well as at various levels within the hydrophobic core.

Comprehensive studies were planned to identify the mechanisms of coagulation structure formation in cream bases.

In addition, the effect of coagulation structure on the release of active substances from cream bases was to be investigated through a series of *in vitro* experiments. For the experiment, two substances were selected: ofloxacin [1] and dexpanthenol [29].

3. Materials and methods

The following excipients were used in the experiments: propylene glycol (Kollisolv® PG) – PG; macrogol cetostearyl ether 20 (Kolliphor® CS 20) – M20CSE; cetostearyl alcohol (Kolliwax CSA 50) – CSA, all of these materials were produced by BASF. Purified water (hereinafter referred to as water) was also used. The oil phase was constituted by a mixture of paraffin liquid (OQEMA GmbH) and paraffin soft (MERCAN KIMYA SAN VE TIC A.S.) (1 : 1) [1]. Pharmacopoeial grade excipients (Ph. Eur.) were used for the experiments [3].

The compositions of the studied cream bases without an oil phase (hereinafter referred to as dispersions) and bases with an oil phase (hereinafter referred to as o/w emulsions) are presented in Tables 1, 2.

Table 1

Composition of the studied dispersions

Constituent	Content (g/100 g) in the base No.:											
	1D	2D	3D	4D	5D	6D	7D	8D	9D	10D	11D	12D
M20CSE	0.5	1.0	2.0	3.0	4.0	5.0	6.0	7.0	8.0	9.0	9.5	10.0
CSA	9.5	9.0	8.0	7.0	6.0	5.0	4.0	3.0	2.0	1.0	0.5	0
PG	9.0	9.0	9.0	9.0	9.0	9.0	9.0	9.0	9.0	9.0	9.0	9.0
Water	81.0	81.0	81.0	81.0	81.0	81.0	81.0	81.0	81.0	81.0	81.0	81.0

Table 2

Composition of the studied emulsions o/w

Constituent	Content (g/100 g) in the base №:											
	1E	2E	3E	4E	5E	6E	7E	8E	9E	10E	11E	12E
M20CSE	0.5	1.0	2.0	3.0	4.0	5.0	6.0	7.0	8.0	9.0	9.5	10.0
CSA	9.5	9.0	8.0	7.0	6.0	5.0	4.0	3.0	2.0	1.0	0.5	0
PG	7.0	7.0	7.0	7.0	7.0	7.0	7.0	7.0	7.0	7.0	7.0	7.0
Water	63.0	63.0	63.0	63.0	63.0	63.0	63.0	63.0	63.0	63.0	63.0	63.0
Paraffin liquid	10.0	10.0	10.0	10.0	10.0	10.0	10.0	10.0	10.0	10.0	10.0	10.0
Paraffin soft	10.0	10.0	10.0	10.0	10.0	10.0	10.0	10.0	10.0	10.0	10.0	10.0

Laboratory samples of bases were obtained by melting the components at approximately 70°C. The resulting mixture was then homogenised using POLYTRON® PT 3100 dispersing unit equipped with a PT-DA 3020/2T dispersing aggregate (Kinematica AG). The samples were subsequently cooled while stirring to ~ 25°C.

The rheological properties of the experimental samples were examined by rotational viscometry [1]. Rheograms were obtained at 25°C [1] using a Rheolab QC rotational viscometer with CC-27 coaxial cylinders (Anton Paar GmbH; RHEOPLUS software version 2.66). The flow behaviour, the yield stress (τ_0), and the apparent viscosity (η) at various shear rates (D_r) or dynamic viscosity (η) were determined from the rheograms.

Electron paramagnetic resonance (EPR) spectroscopy was employed to study the microstructure of the aggregates of surfactant and CSA [25]. The following spin probes were used:

– **probe 1**: 4-Palmitamido-2,2,6,6-tetramethylpiperidine-1-oxyl (M_r 409.67; CAS [22977-65-7]);

– **probe 2**: 4-(N,N-dimethyl-N-hexadecyl)ammonio-2,2,6,6-tetramethylpiperidine-1-yloxy iodide (M_r 551.65; CAS: [114199-16-5]);

– **probe 3**: 5-Doxyl Stearic acid, ammonium salt (M_r 401.61; CAS: [2315262-05-4]) (5-DSA, NH_4 salt);

– **probe 4**: 16-Doxyl Stearic acid (M_r 384.57; CAS [53034-38-1]) (16-DSA).

The spin probes were added to the studied systems at a concentration of 10^{-4} mol/l. The EPR spectra were recorded at 25°C using the ESR Spectrometer CMS8400 («Adani»; software EPRCMD).

By the EPR spectra, which were triplets, the peak heights at the low-field (h_{+1}), central (h_0) and high-field (h_{-1}) components, as well as the linewidth at the low-field (ΔH_{+1}) and central (ΔH_0) components were determined. The rotational correlation times of the spin probes (τ_{+1}, τ_{-1}, $\tau_{\pm1}$) and the anisotropy parameter (ε) were calculated using the following equations:

$$\tau_{+1} = \left(\sqrt{\frac{h_0}{h_{+1}}} - 1\right) \cdot \Delta H_0 / 2 \cdot 10^8; \quad (1)$$

$$\tau_{-1} = \left(\sqrt{\frac{h_0}{h_{-1}}} - 1\right) \cdot \Delta H_0 / 3.6 \cdot 10^9; \quad (2)$$

$$\tau_{\pm1} = \left(\sqrt{\frac{h_{+1}}{h_{-1}}} - 1\right) \cdot \Delta H_{+1} \cdot 6.65 \cdot 10^{-10}; \quad (3)$$

$$\varepsilon = \frac{\sqrt{h_0/h_{+1}} - 1}{\sqrt{h_0/h_{-1}} - 1}. \quad (4)$$

According to Stokes' equation, the rotational correlation time (τ) is directly proportional to the viscosity (η) of the local microenvironment of the spin probe and inversely proportional to the absolute temperature (T):

$$\tau = \left(4 \cdot \pi \cdot R^3 \cdot \eta\right) / \left(3 \cdot k \cdot T\right). \quad (5)$$

The A_N constant, which characterizes the polarity of the radical's environment, was determined as the distance (in mT) between the central and high-field components.

In the case of the EPR spectra for probes 3 and probe 4, A_N constant and the order parameter (S) were calculated after determining the hyperfine splitting constants $A_{\parallel}$ and $A_{\perp}$ according to the following equation:

$$A_N = (A_{\parallel} + 2A_{\perp}) / 3; \quad (6)$$

$$S = \frac{A_{\parallel} - A_{\perp}}{A_{\parallel} + 2A_{\perp}} \times 1.66. \quad (7)$$

A circulating thermostat Julabo F12-ED («Julabo Labortechnik GmbH») was used to maintain the required temperature.

In the course of *in vitro* experiments, the release of ofloxacin and dexpanthenol was studied. The investigation focused on creams containing 0.1% ofloxacin in bases numbered 4D and 4E (Tables 1, 2), a 0.1% ofloxacin solution in a mixed solvent *water – PG* (9 : 1), as well as a 5% aqueous solution of dexpanthenol and Bepanthen® Plus cream (batch GP02ZH1)

The release of active substances from creams and solutions was determined by dialysis through a semipermeable cellulose membrane at (32 ± 0.5)°C using a Vertical Diffusion Cell System HDT 1000 (COPLEY Scientific, UK). A quantity of 0.5 g of cream or solution was placed into the donor chamber. The contact area with the membrane was 1.00 cm^2. The volume of receptor medium (water) was 6.6 ml, the stirring frequency was 600 rpm, and the sample volume was 0.3 ml.

The quantity of an active substance released into water per unit of membrane area (1 cm^2) was determined. The rate of active substance release (b), correlation coefficient (R), coefficient of determination (R^2), cumulative content (A) (at the time point 6 hours), and recovery (at the time point 6 hours) were calculated.

The procedures for the *in vitro* release test (IVRT) were validated in accordance with established approaches [32, 33].

The quantification of ofloxacin or dexpanthenol was conducted by liquid chromatography, employing the analytical procedures described in the papers [34] and [35], respectively.

4. Research results

The rheological characteristics and apparent viscosity of cream bases at 25°C were contingent on the mass ratio between M20CSE and CSA (Fig. 1, 2).

As the mass fraction of M20CSE increased, the rheological parameters rose and reached their peak values at mass ratios between M20CSE and CSA of approximately 3.0:7.0 (Fig. 2). It was shown that, up to a certain mass ratio of M20CSE to CSA, the cream bases exhibited plastic flow (Fig. 1). Hysteresis loops are evident in the rheograms (Fig. 1), indicating that when shear stress was applied, the apparent viscosity decreased and did not immediately recover. At certain ratios of M20CSE to CSA, the flow behavior of the bases shifted toward Newtonian flow (Fig. 1). The resulting o/w emulsions demonstrated a liquid consistency and experienced rapid separation.

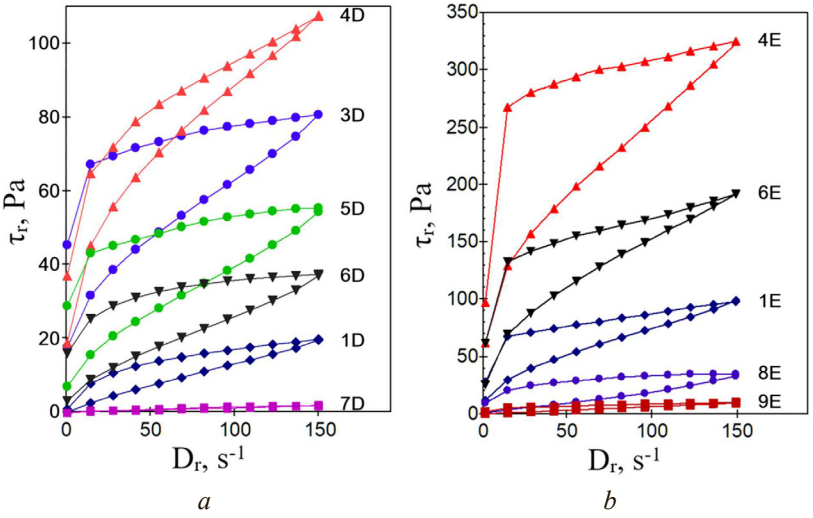

Fig. 1. Rheograms of cream bases with M20CSE and CSA at different ratios: *a* – rheograms of dispersions (see Table 1 for markings); *b* – rheograms of emulsions o/w (see Table 2 for markings)

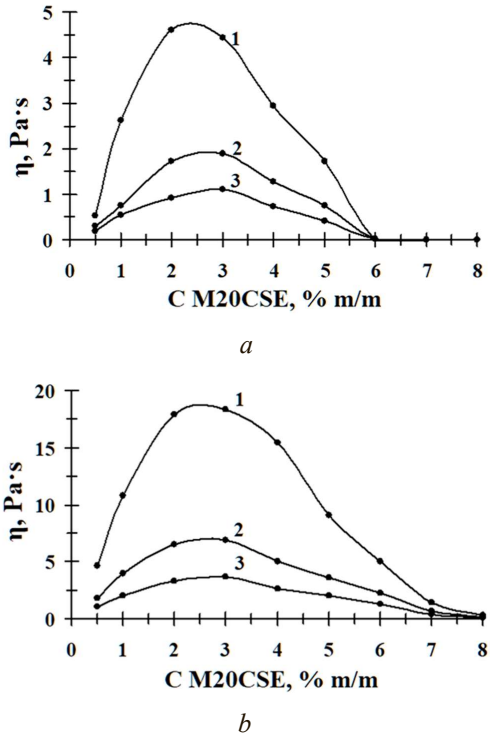

Fig. 2. Dependence of apparent viscosity (η) of bases on the content of M20CSE (C) at shear rate (D_r) 14.6 s^{-1} (1), 48.6 s^{-1} (2), 82.1 s^{-1} (3) and 25°C: *a* – apparent viscosity of dispersions; *b* – apparent viscosity of emulsions o/w

The apparent viscosity of dispersions containing M20CSE and CSA in ratios of 2.0 : 8.0 to 3.0 : 7.0 was approximately 4 times lower than the apparent viscosity

of o/w emulsions (Fig. 2). However, both dispersions and o/w emulsions with this emulsifying composition could be used as cream bases. In order to exercise control over the properties of such bases, it was first necessary to develop a comprehensive understanding of how the structure of mixed aggregates of M20CSE and CSA changed at the supramolecular level in response to variations in their mass ratio. The objective was to comprehend the mechanisms that initiated alterations in the rheological parameters of dispersed systems.

The EPR spectra of the hydrophobic spin probe 1 are presented in Fig. 3. The alkyl chain of probe 1 was localised in the non-polar part of the mixed aggregates M20CSE and CSA, and the nitroxyl radical was localised in their polar part.

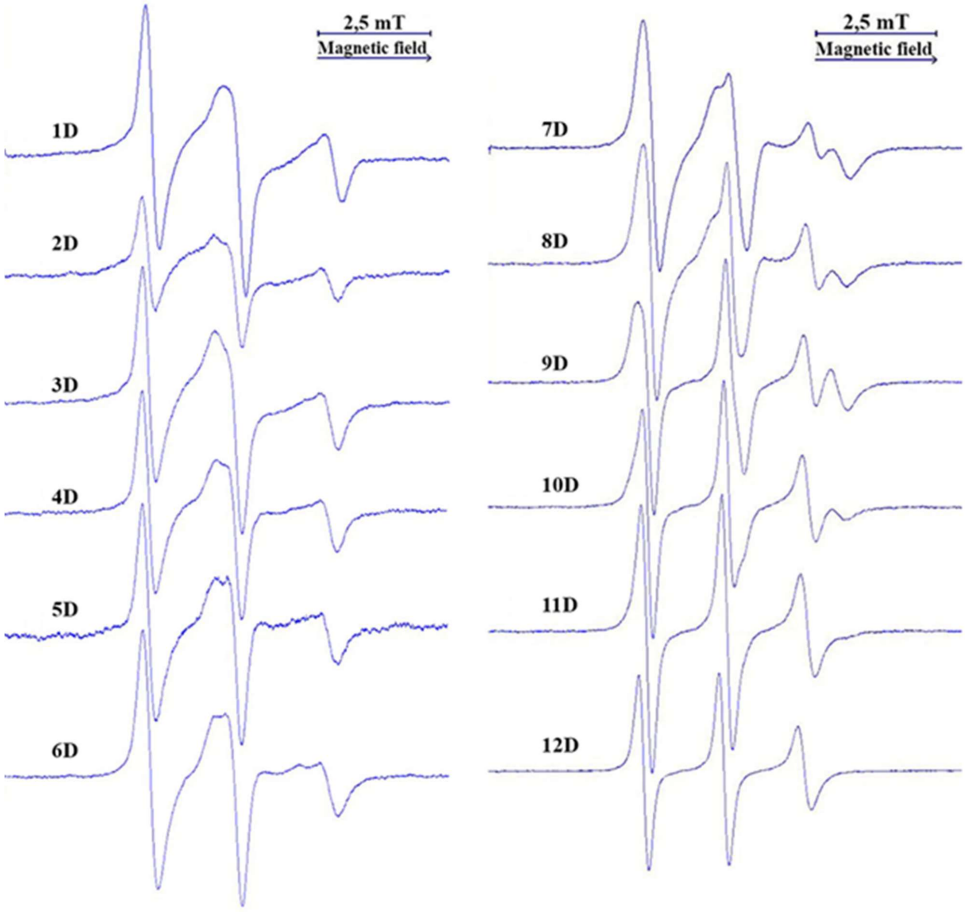

Fig. 3. EPR spectra of probe 1 in dispersions at 25°C (in Fig. 3–6, the EPR spectra markings correspond to the markings in Table 1)

In dispersions No. 1D – 6D, the EPR spectra of probe 1 were superpositions of a singlet and two triplets; in dispersions No. 7D – 10D, they were superpositions of two triplets, and in dispersions No. 11D and No. 12D, the EPR spectra were triplets. The EPR spectra indicated that lateral phase separation occurred in the M20CSE and CSA aggregates in dispersions No. 1D – 10D. In the domains formed by CSA in dispersions No. 1D – 6D, CSA molecules were found to be very densely packed. In this phase, probe 1 provided two EPR spectra, namely: a singlet caused by exchange broadening due to the contact of nitroxyl radicals with each other through dense packing, and a triplet with an isotropic constant A_N of approximately 2.1 mT. The second is a triplet with an isotropic constant A_N of approximately 2.1 mT. This finding suggests that the nitroxyl radical of probe 1 was localized in a hydrophilic dispersion medium. The domain formed from CSA molecules at the interface with the dispersion medium was hypothesised to have a solid consistency; the tight packing of CSA molecules prevented hydrophobic hydration of their alkyl chains.

Based on the EPR spectra of probe 1 in dispersions No. 7D – 10D, it was possible to determine the isotropic constant A_N of the EPR spectra of probe 1 in the phase of M20CSE, which was approximately 1.64 mT. This indicated that the nitroxyl radical of probe 1 was localized in the polyethylene oxide chains of M20CSE. It was observed that the greater the specific proportion of M20CSE, the lower the signal intensity with a high isotropic constant of ~2.1 mT, and the greater the signal intensity with a value of $A_N \approx 1.64$ mT. It was demonstrated that an increase in the specific fraction of M20CSE resulted in a decrease in signal intensity with a high isotropic constant of ~ 2.1 mT, and an increase in signal intensity with a value of $A_N \approx 1.64$ mT. In dispersion No. 11D, molecules of CSA and probe 1 were distributed almost uniformly in the plane of the aggregates containing 90% M20CSE. The solubilised CSA molecules contributed to the increase in the microviscosity of M20CSE micelles in dispersion No. 11D by approximately 1.43 times compared to system No. 12D; the values of $\tau_{\pm1}$ increased from 0.77 ns to 1.10 ns.

The presence of a singlet in the EPR spectra of probe 1 is characteristic for dispersed systems with plastic flow and thixotropic properties. The transition to EPR spectra that were superpositions of only two triplets indicated a transition to dispersed systems with Newtonian flow (Fig. 1, *a*, 3).

Thus, one of the reasons for the formation of coagulation structures is the lateral distribution of phases and the presence of a certain quantity of solid CSA domains. However, sample No. 1, containing 9.5% CSA and 0.5% M20CSE, with the largest quantity of solid domains, was characterised by low rheological parameters, which increased with an increase in the content of hydrophilic surfactant M20CSE to 2–3%. This can be explained by

the fact that, within a dispersion medium where water structure was dominant, mixed aggregates of M20CSE and CSA must be hydrated to some extent. The presence of a non-ionic surfactant ensured this hydration process. The graphs, which illustrate the dependence of rheological parameters on the composition of emulsifiers (Fig. 2, *a*), demonstrate extremes that are associated with two processes: an increase in the hydration of aggregates, on the one hand, and a decrease in the quantity of CSA solid domains, on the other.

A hydrophilic spin probe 2, which is a cationic surfactant, was utilised in the experiment. The alkyl chain of probe 2 was also localised in the non-polar regions of the aggregates, and the nitroxyl radical was localised in their polar parts.

The EPR spectra of probe 2 in dispersions No. 1D–5D are the superpositions of two triplets, which were separated in the high-field. The hydrophilic properties of probe 2 enabled the prevention of exchange expansion, even in circumstances where its molecules were localised in CSA domains.

The absence of a singlet in the spectra, which were superpositions, facilitated their processing compared to the spectra of probe 1. The isotropic constant A_N of the first signal was 1.73 mT, and A_N of the second signal was approximately 1.62 mT. A decline in the CSA content resulted in a decrease in the proportion of the signal exhibiting a higher A_N value. According to the EPR spectra of probe 2, the lateral phase distribution occurred in the aggregates of M20CSE and CSA in dispersions No. 1D–5D. In the high-field component of the EPR spectrum in dispersion No. 6D, the superposition of two spectra remains discernible. Some parameters of the triplet EPR spectra of probe 2 in dispersions No. 7D–12D were calculated (Fig. 4, Table 3).

The decrease in the values of isotropic constant A_N of the EPR spectra of spin probe 2 from 1.68 mT to 1.62 mT, coupled with a decrease in CSA content, is likely indicative of a uniform distribution of M20CSE and CSA in their aggregates. A decline in CSA content resulted in a decrease in the rotational correlation times of probe 2. In the case of dispersion No. 7D, the value of $\tau_{\pm1}$ was 1.72 ns, i.e., close to the slow rotation; for dispersion No. 12D, this value decreased to 1.29 ns. Furthermore, the anisotropy parameter ε also decreased from 0.20 to 0.08. It can be posited that, in dispersions No. 1D–5D, the molecules of the spin probe 2 rotate very slowly within the CSA domains.

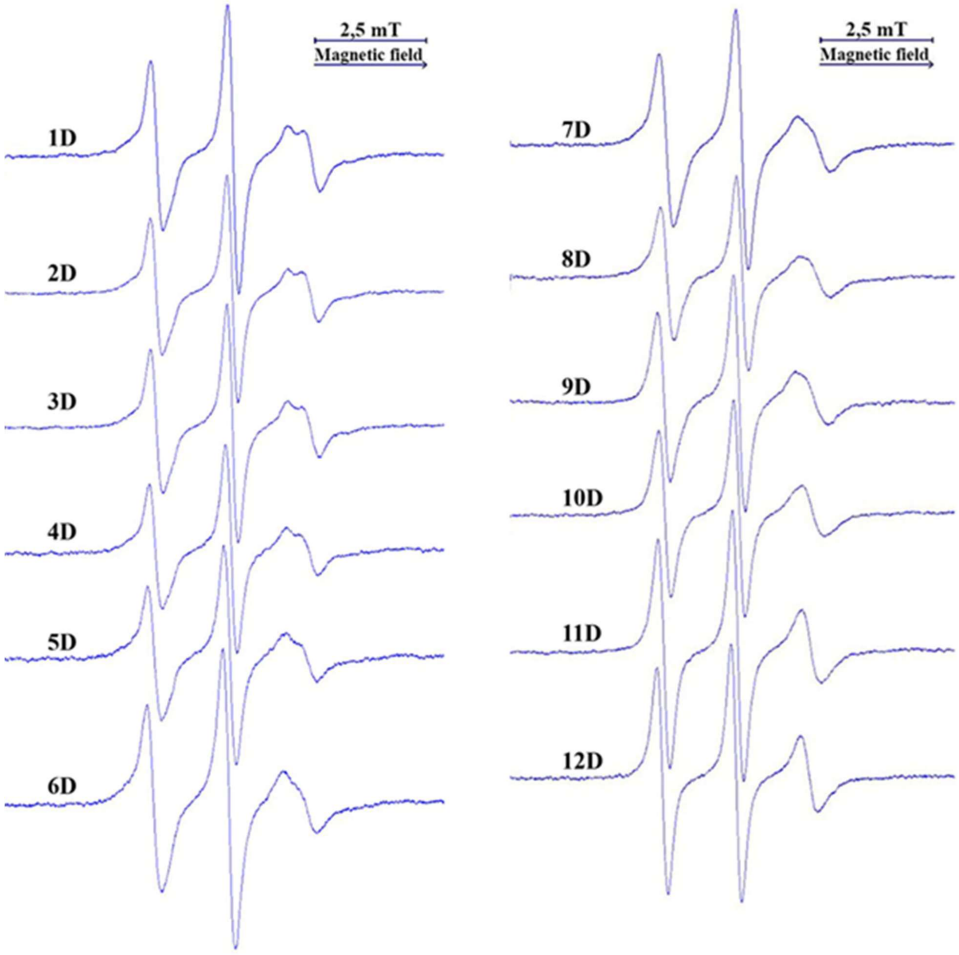

Fig. 4. EPR spectra of probe 2 in dispersions at 25°C

Table 3

Parameters of the EPR spectra of spin probe 2 in dispersions No. 7D–12D at 25°C

Dispersion	M20CE content, %	CSA content, %	τ_{+1}, ns	τ_{-1}, ns	$\tau_{\pm1}$, ns	ε	A_N, mT
No. 7D	6.0	4.0	> 2.0	0.88	1.72	0.20	1.68
No. 8D	7.0	3.0	> 2.0	0.87	1.69	0.18	1.66
No. 9D	8.0	2.0	> 2.0	0.83	1.58	0.17	1.64
No. 10D	9.0	1.0	1.90	0.80	1.45	0.13	1.63
No. 11D	9.5	0.5	1.18	0.70	1.40	0.09	1.62
No. 12D	10.0	0	0.87	0.62	1.29	0.08	1.62

The results of studies conducted with probe 2 also demonstrated a correlation with the dependence of the rheological properties of the dispersions on the ratio of M20CSE to CSA. Furthermore, the results obtained indicated lateral phase separation in the aggregates of M20CSE and CSA, as well as the presence of solid CSA domains.

Subsequent experiments were conducted using spin probe 3, whose alkyl chain localized in the non-polar region of the aggregates, and the doxyl radical also localized in the non-polar region, at a level of approximately the 5th carbon atom.

The EPR spectra of spin probe 3 in dispersions with high rheological parameters were anisotropic, and

high values of the order parameter S were characteristic for them: 0.47 for dispersion No. 1D, 0.48 for dispersion No. 2D, 0.49 for dispersions No. 3D and No. 4D, 0.48 for dispersion No. 5D. The EPR spectra of spin probe 3 in dispersions with high rheological parameters were anisotropic, and high values of the order parameter *S* were characteristic for them: 0.47 for dispersion No. 1D, 0.48 for dispersion No. 2D, 0.49 for dispersions No. 3D and No. 4D, 0.48 for dispersion No. 5D. The doxyl radical was found in a non-polar environment, as evidenced by the isotropic constants of the EPR spectra, which were approximately 1.49 mT.

A further increase in the specific fraction of M20CSE and a decrease in the CSA content resulted in the transformation of the EPR spectra of probe 3 into triplets. The order parameter S of the EPR spectrum of probe 3 in dispersion No. 6D decreased to 0.29, and averaged 0.22 for dispersions No. 7D–12D.

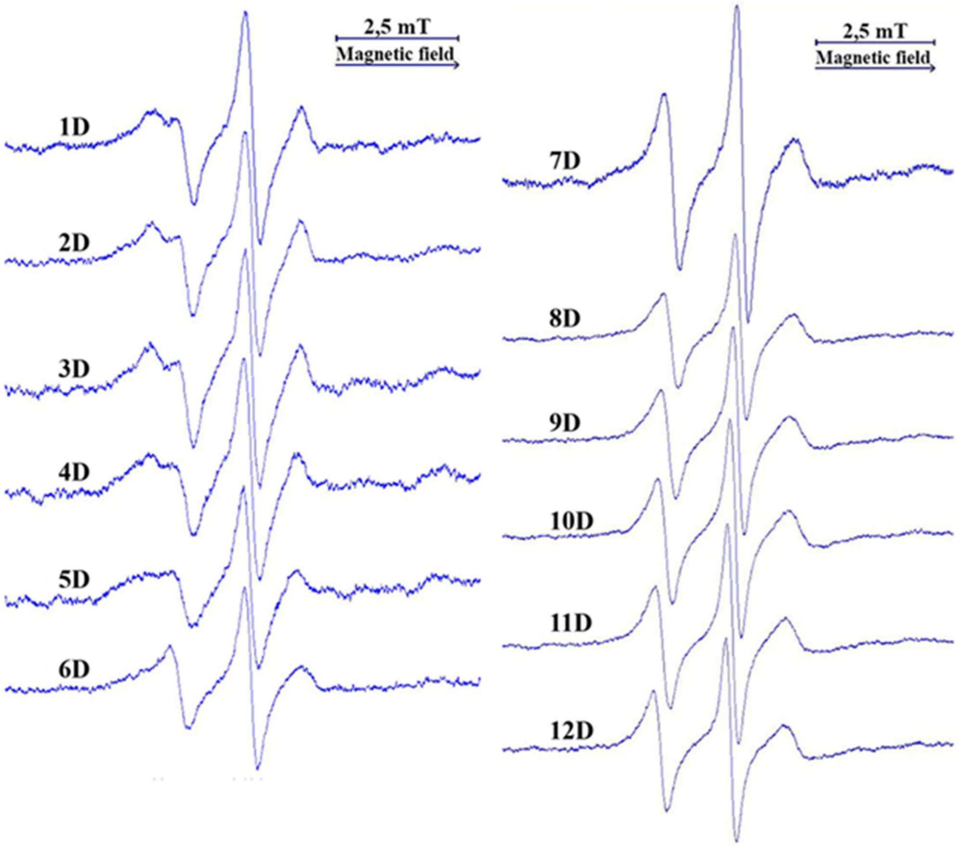

Fig. 5. EPR spectra of probe 3 in dispersions at 25°C

Therefore, at the level of the 5th carbon atom of the alkyl chains, according to the EPR spectra of probe 3 in dispersions No. 3D and No. 4D, which were characterised by the highest apparent viscosity, there was a very dense and ordered packing of alkyl chains in the mixed aggregates of M20CSE and CSA. This packing exhibited substantial disparities in density and orderliness when compared to that observed in dispersions No. 6D – 12D with the higher content of M20CSE. In dispersion No. 8D, the rotational correlation times of probe 3 exhibited characteristics indicative of systems with a liquid consistency (τ_{-1} = 1.07 ns, $\tau_{\pm1}$ = 1.53 ns). In particular, the EPR spectrum of probe 3 in liquid paraffin at 37°C was characterised by the following parameters: τ_{-1} = 0.94 ns, $\tau_{\pm1}$ = 1.61 ns. Due to the liquid consistency of the mixed aggregates, coagulation structures did not form in the water-glycol dispersion medium, where the structure of water prevailed.

The alkyl chain of probe 4 is located in the non-polar region of the aggregates, and the doxyl radical is also located in the non-polar part, approximately at the level of the 16th carbon atom.

At ratios of M20CSE to CSA of 0.5:9.5 and 1.0:9.0, the EPR spectra of probe 4 were superpositions of the anisotropic spectrum and triplet (Fig. 6), indicating lateral phase distribution at the level of 16th carbon atoms. At ratios of M20CSE to CSA of 2.0:8.0 and 3.0:7.0, at which the maximum values of the apparent viscosity of dispersed systems were observed (Fig. 2, *a*), the EPR spectra of probe 4 in these systems were anisotropic with high values of order parameters *S*, which were 0.43 and 0.45, respectively. At ratios of M20CSE to CSA of 4.0:6.0 and 5.0:5.0, the EPR spectra of probe 4 were once again superpositions of two spectra: an anisotropic one with parameter *S* 0.45 and a triplet. It is evident that, at these certain ratios M20CSE and CSA, lateral phase distribution occurred at the level of the 16th carbon atom. As the fraction of M20CSE increased, the EPR spectra gradually transformed into triplets (Fig. 5).

In the EPR spectra of probe 4 in dispersions No. 7D and No. 8D, triplets were dominant (Fig. 6), i.e., lateral phase distribution at the level of the 16th carbon atom of alkyl chains practically did not occur. This finding aligned with the change of the flow behaviour of dispersed systems from plastic flow to Newtonian (Fig. 1a). It was characteristic for the EPR spectra of probe 4 that at a ratio of M20CSE to CSA of 7.0:3.0 (dispersion No. 8D) and with a further decrease in the CSA content, the parameters of the EPR spectra practically did not change (Table 4).

The cores of the spherical micelles formed by M20CSE at the 16th carbon atom level at 25°C were in a liquid state, as evidenced by the parameters of the EPR spectra of spin probe 4 in dispersion No. 12D (Table 4). The doxyl radical was in a non-polar environment, as indicated by the low values of isotropic constant of the EPR spectra (A_N = 1.49 mT). The liquid consistency of

the micelles at this level was confirmed by the values of the EPR spectrum parameters of probe 4 in liquid paraffin at 25°C: τ_{+1} = 0.43 ns, τ_{-1} = 0.58 ns, and $\tau_{\pm 1}$ = 1.28 ns.

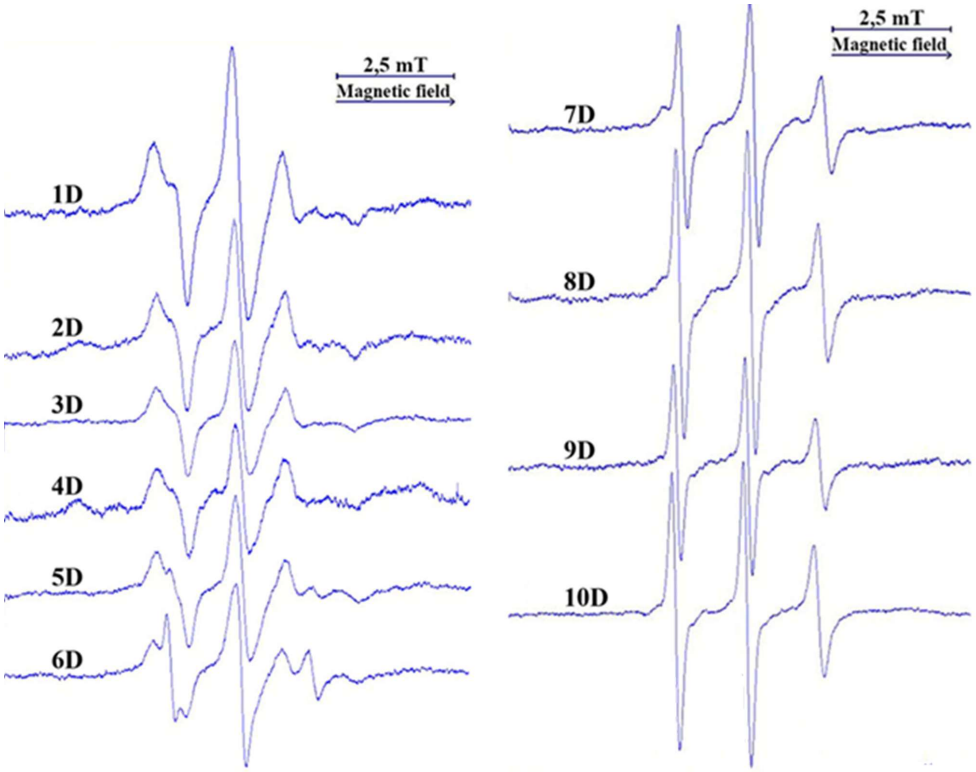

Fig. 6. EPR spectra of probe 4 in dispersions at 25°C

Table 4

Parameters of the EPR spectra of spin probe 4 in dispersions No. 7D–12D at 25°C

Dispersion	Content M20CE, %	Content CSA, %	τ_{+1}, ns	τ_{-1}, ns	$\tau_{\pm 1}$, ns	ε	A_N, mT
No. 8D	7.0	3.0	0.56	0.28	0.60	0.11	1.49
No. 9D	8.0	2.0	0.52	0.28	0.54	0.10	1.49
No. 10D	9.0	1.0	0.50	0.29	0.59	0.10	1.49
No. 11D	9.5	0.5	0.56	0.29	0.62	0.11	1.49
No. 12D	10.0	0	0.56	0.31	0.58	0.10	1.49
			0.54 ± 0.035	0.29 ± 0.015	0.59 ± 0.037	0.104 ± 0.007	1.49 ± 0

Unlike the spherical micelles, the alkyl chains at the 16th carbon atom in dispersions No. 3D and No. 4D underwent dense and ordered packing. This indicates that the mixed aggregates M20CSE and CSA were non-spherical in configuration. Fig. 7 illustrates the difference in the EPR spectra of the four spin probes in these dispersed systems. One dispersion exhibited plastic flow behaviour and thixotropy, while the other was a Newtonian liquid (Fig. 1, *a*). In dispersion No. 11D, the M20CSE and CSA molecules were evenly distributed within the plane of the mixed aggregates, as can be seen from the EPR spectra, which were triplets.

In the case of dispersions with a maximum apparent viscosity (Fig. 2, *a*), the non-polar part of the associates was in a solid-like state and highly ordered along the entire length of the alkyl chains. Lateral phase separation was only observed at the interface with the dispersion medium, where solid domains formed by CSA were located next to liquid domains of M20CSE, which ensured the hydration of mixed aggregates. The EPR spectra of four fatty acid-based spin probes differed significantly in the case of such mixed aggregates compared to the spectra in the case of spherical micelles (Fig. 7).

Similar studies were conducted on cream bases with an oil phase, i.e., o/w emulsions. The EPR spectra of the hydrophobic spin probe 1 in these emulsions are presented in Fig. 8 (Table 2 for markings).

The EPR spectra of probe 1 in emulsions No. 1E–4E were superpositions of a singlet and two triplets. In emulsions No. 5E–9E, the spectra were superpositions of two triplets. In emulsion No. 10E, the EPR spectrum was a triplet (Fig. 8). These spectra indicated a lateral phase distribution within the adsorption layers in the case of emulsions No. 1E–9E. An increase in the M20CSE content resulted in a decrease in the signal intensity in the high-field component with a high A_N value of ~ 2.15 mT, indicating a reduction in the quantity of CSA solid-like domains.

The highest apparent viscosity was observed in emulsions No. 3E and No. 4E (Fig. 2, *b*). At a mass ratio of M20CSE and CSA of 3.0 : 7.0, the optimal balance was achieved between the hydration of the adsorption layers and the fraction of CSA domains with dense packing. In the case of emulsions No. 5E, No. 6E and No. 7E, the singlet disappeared in the EPR spectra (Fig. 8), and their apparent viscosity decreased (Fig. 2, *b*). In the case of emulsion No. 10E, the M20CSE and CSA molecules were uniformly distributed across the adsorption layers. According to the parameters of the EPR spectrum of probe 1 (τ_{-1} = 0.54 ns, $\tau_{\pm 1}$ = 1.33 ns), these layers had a liquid consistency. In this case, coagulation structures were not formed, the physical stabilization factor was lost, and the emulsions quickly separated during storage.

The EPR spectra of four spin probes in emulsion base No. 4E, which exhibited the highest apparent vis-

cosity, and in emulsion No. 10E, which had a liquid consistency and separated during storage, are presented in Fig. 9.

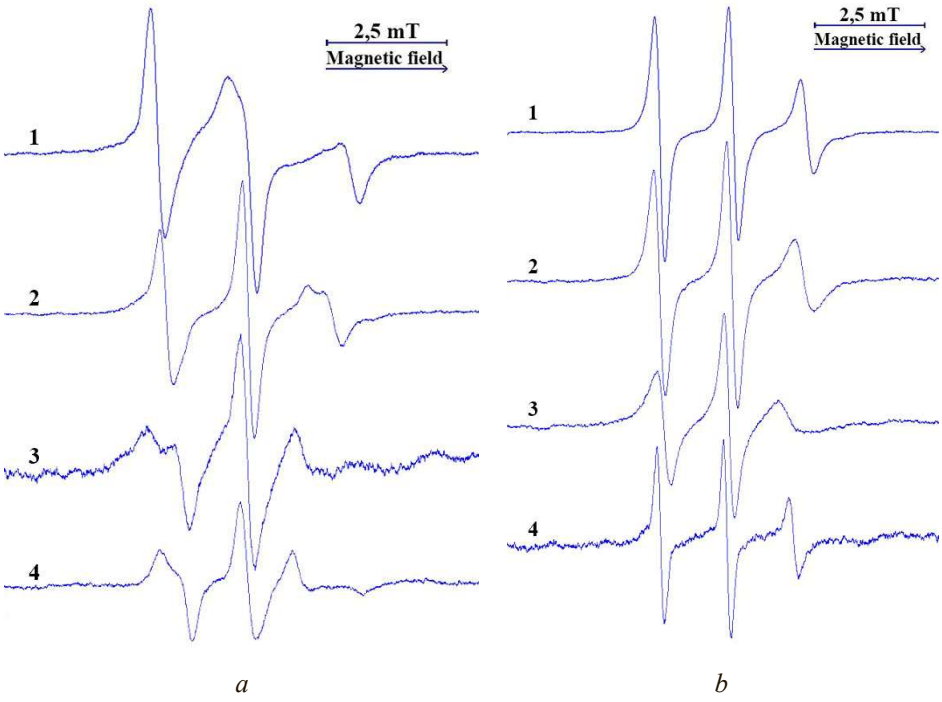

a *b*

Fig. 7. EPR spectra of probes 1, 2, 3, 4 in the different dispersions at 25°C: *a* – No. 3D (M20CSE i CSA 2.0:8.0); *b* – No. 11D (M20CSE i CSA 9.5:0.5)

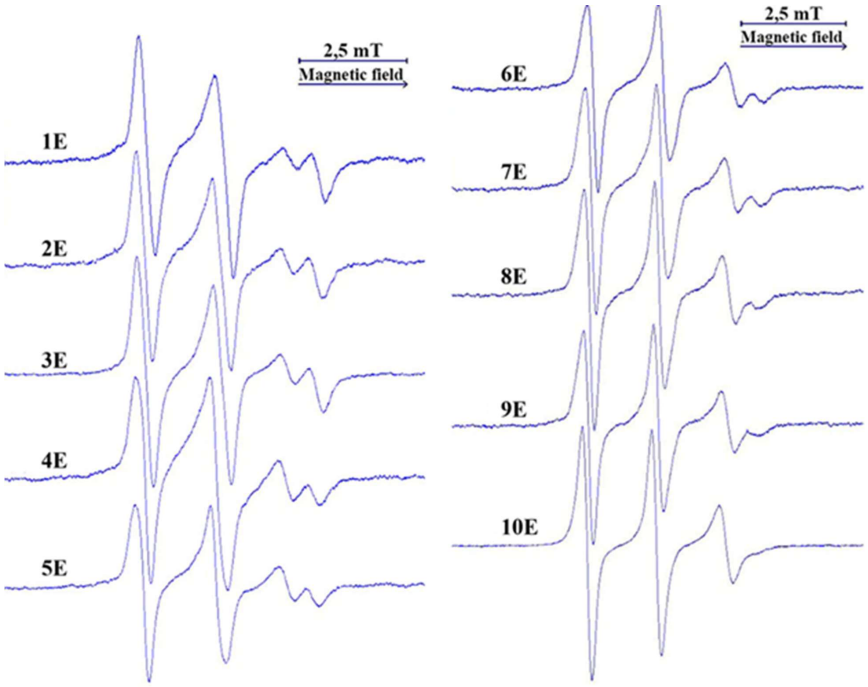

Fig. 8. EPR spectra of probe 1 in o/w emulsions at 25°C (In Fig. 8, 9, the EPR spectra markings correspond to the markings in Table 2)

The EPR spectra of probe 1 in emulsion No. 4E were found to be superposition of a singlet and two triplets, which were separated in the high-field component (Fig. 9, *a*). This finding indicates lateral phase separation in the adsorption layers. The EPR spectrum of probe 2 in emulsion No. 4E exhibited a superposition of two triplets. In the case of emulsion No. 10E, which was a Newtonian liquid, EPR spectra of probes 1 and 2 were triplets.

The EPR spectrum of spin probe 3 in emulsion No. 4E was anisotropic, exhibiting a high value of order parameter $S \approx 0.47$. An increase in the M20CSE content resulted in a decrease in the values of S parameter to 0.42 in emulsion No. 6E and to 0.41 in emulsion No. 7E. This decrease correlated with a reduction in the apparent viscosity of the emulsions (Fig. 2, *b*). At a mass ratio of M20CSE to CSA of 9.0 : 1.0 in liquid emulsion No. 10E, the EPR spectrum of probe 3 was a triplet (Fig. 9, *b*).

The EPR spectra of probe 4 to emulsion No. 4E were superpositions of two triplets separated in the high-field component (Fig. 9, *a*), indicating lateral phase separation at the level of the 16th carbon atom. The doxyl radical of probe 4 was located in a nonpolar environment, as confirmed by the values of isotropic constant of the EPR spectra, which were found to be approximately 1.42–1.49 mT. The phase separation was presumably caused by the formation of dense domains by some of the alkyl chains, while others dissolved in the oil phase exhibited greater rotational freedom.

A decrease in the apparent viscosity of emulsions (emulsions No. 5E–10E) (Fig. 2, *b*) was accompanied by a transformation of the EPR spectra into triplets. The parameters of these EPR spectra indicated a liquid consistency of the adsorption layers at the level of the 16th carbon atom. Thus, in the case of the EPR spectrum of probe 4 in emulsion No. 10E (Fig. 9, *b*), τ_{+1} was 0.60 ns, τ_{-1} was 0.33 ns, and $\tau_{\pm1}$ was 0.70 ns.

The present study investigated the influence of the coagulation structure in cream bases No. 4D and No. 4E on their performance characteristics regarding the release of the active ingredient ofloxacin from these bases in experiments *in vitro* (*in vitro* release test). The study was conducted at 32°C. An increase in temperature by 7°C did not have a sig-

nificant effect on the configuration and parameters of the EPR spectra of spin probes in these cream bases. Thus, the EPR spectra of spin probe 3 remained anisotropic; at temperatures of 25°C and 32°C, the values of order parameter S in cream base No. 4D were 0.49 and 0.48, respectively, and in cream base No. 4E, they were 0.47 and 0.45, respectively.

A comparative study was conducted on the release of ofloxacin from cream bases No. 4D and No. 4E, as well as from mixed solvent *PG – water* (1 : 9).

The release parameters of ofloxacin were significantly higher in the case of *PG – water* solvent (1 : 9) than from cream bases (Fig. 12, Table 5). The kinetics and release parameters of ofloxacin from cream bases No. 4D (without oil phase) and No. 4E (with oil phase) were found to be almost identical (Fig. 12 and Table 5).

Bepanthen® Plus cream contains 5% dexpanthenol. The base of this cream is o/w emulsion, which is characterized by a plastic flow type and thixotropic properties (Fig. 13). Gas chromatography was utilized to analyze the formulation of the preparation, revealing the presence of 3.6% cetyl alcohol and 2.4% stearyl alcohol. Liquid chromatography was used to ascertain that the concentration of macrogol 40 stearate is 3.0%.

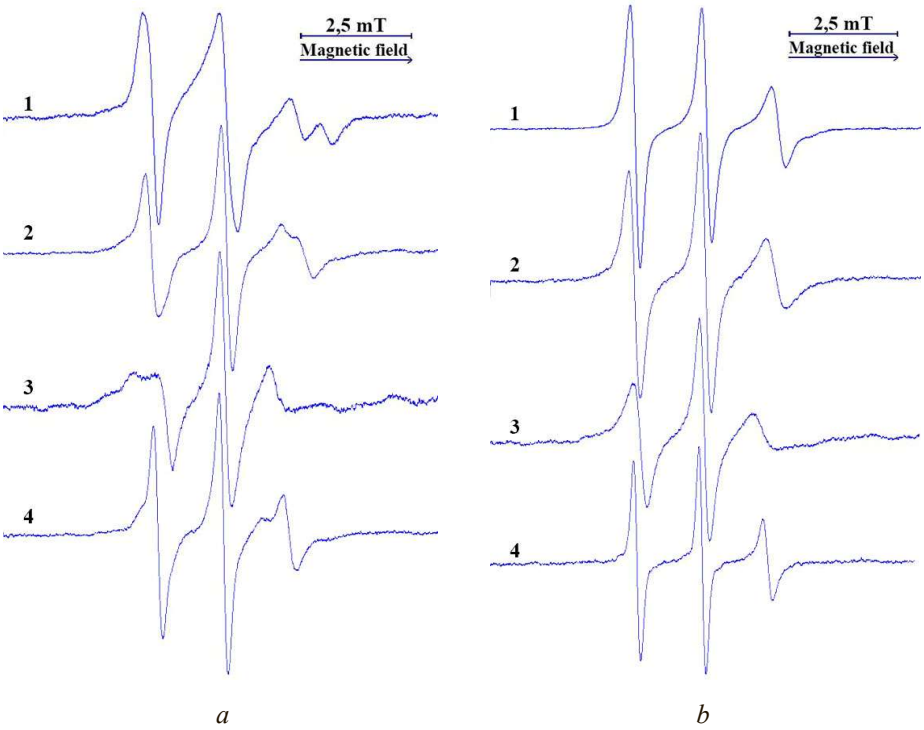

a *b*

Fig. 9. EPR spectra of probes 1, 2, 3, 4 in the different o/w emulsions at 25°C: *a* – No. 4E (M20CSE i CSA 3.0:7.0); *b* – No. 10E (M20CSE i CSA 9.0:1.0)

Table 5

Ofloxacin release parameters

Parameter	Value in the case of release from:		
	0.1% solution	dispersion No. 4D	o/w emulsion No. 4E
Release rate (*b*), μg/cm²/h$^{-1/2}$	192.48 ± 9.63 SD: 7.7550	25.42 ± 3.17 SD: 2.5498	24.76 ± 1.92 SD: 1.5426
Correlation coefficient (*R*)	0.98580	0.99833	0.99940
Coefficient of determination (R^2)	0.97180	0.99666	0.99880
Cumulative amount (*A*) (at the time point 6 h), μg/cm²	406.67 ± 18.23 SD: 14.6817	55.49 ± 6.20 SD: 4.9943	58.35 ± 2.90 SD: 2.3366
Recovery (at the time point 6 h),%	81.33 ± 3.65 SD: 2.94	11.10 ± 1.24 SD: 1.00	11.67 ± 0.58 SD: 0.47

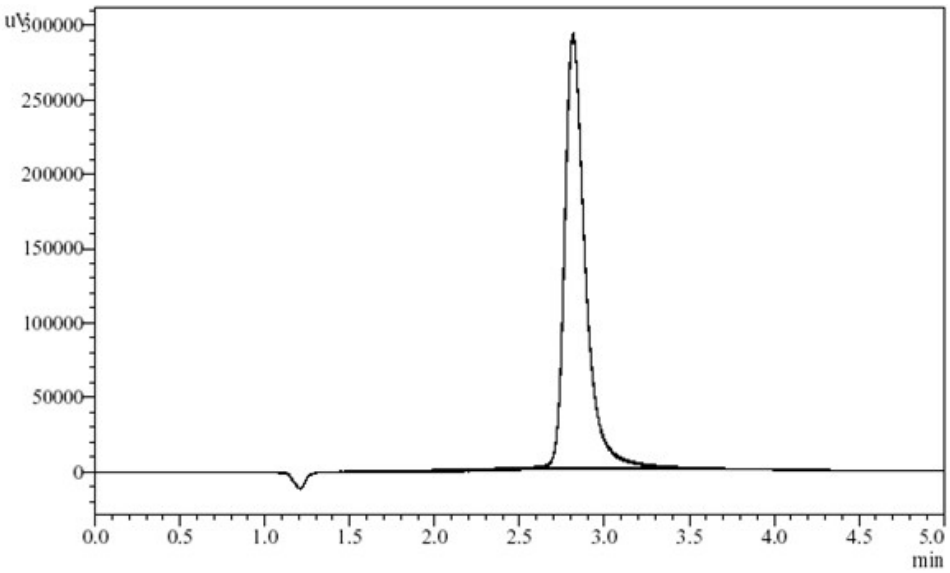

Fig. 10. Chromatogram of the reference solution with ofloxacin content 26.50 μg/ml for the *in vitro* release test

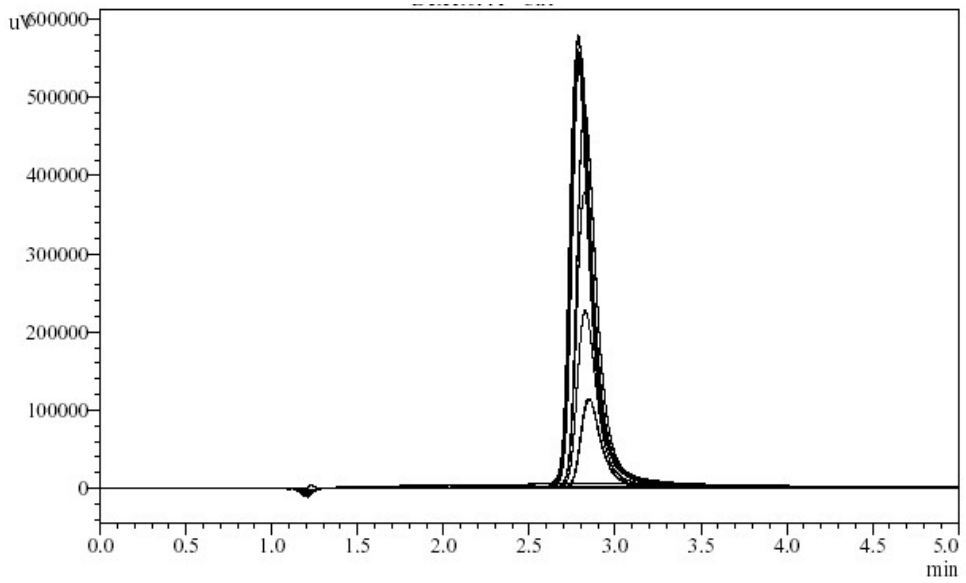

Fig. 11. Representative chromatograms of dialysate samples obtained during the *in vitro* release test for ofloxacin

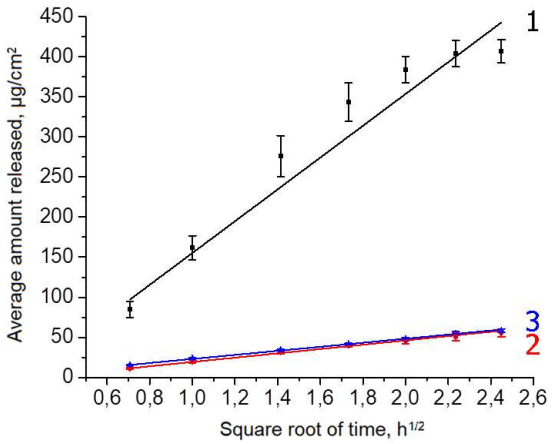

Fig. 12. Ofloxacin release rate plots in the case of release from: 1 – 0.1% solution; 2 – dispersion No. 4D; 3 – o/w emulsion No. 4E

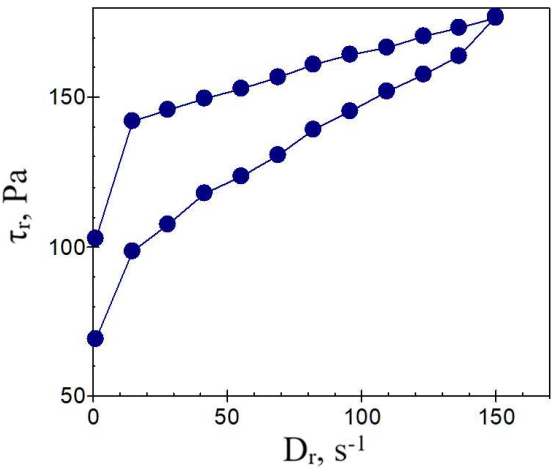

Fig. 13. Rheogram of Bepanthen® Plus cream at 25°C

In the case of Bepanthen® Plus cream, the EPR spectrum of probe 1 exhibited a superposition of a singlet and two triplets, while the EPR spectrum of probe 2 manifested a superposition of two triplets. The EPR spectrum of probe 3 was anisotropic, with a high value of order parameter S, which was 0.54. With regard to probe 4, its EPR spectrum exhibited a superposition of two triplets that were not fully separated in the high-field component (Fig. 14).

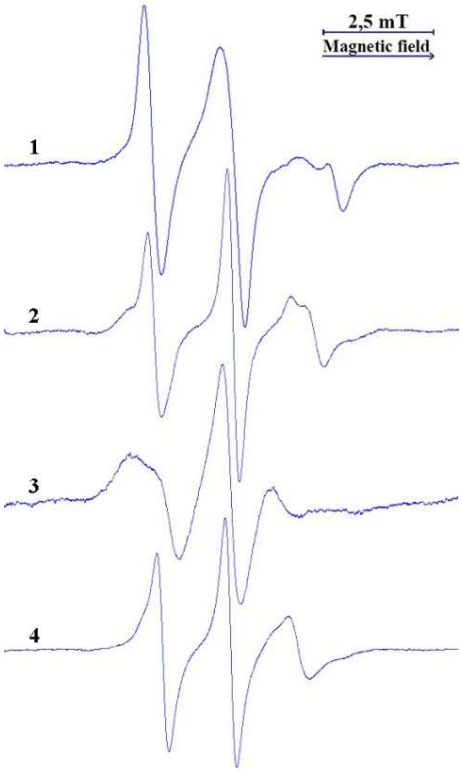

Fig. 14. EPR spectra of spin probes 1, 2, 3 and 4 in Bepanthen® Plus cream at 25°C

The release parameters of dexpanthenol were found to be considerably higher in the case of a 5% aqueous solution compared to Bepanthen® Plus cream (Fig. 15, Table 6).

Table 6

Dexpanthenol release parameters

Parameter	Value in the case of release from:	
	5% solution	Bepanthen® Plus cream
Release rate (b), μg/cm²/h$^{-1/2}$	7.33 ± 0.22 SD: 0.177	1.43 ± 0.07 SD: 0.057
Correlation coefficient (R)	0.98953	0.99968
Coefficient of determination (R^2)	0.97917	0.99936
Cumulative amount (A) (at the time point 6 h), μg/cm²	16.69 ± 0.75 SD: 0.605	3.53 ± 0.19 SD: 0.153
Recovery (at the time point 6 h),%	66.75 ± 3.01 SD: 2.42	14.14 ± 0.76 SD: 0.61

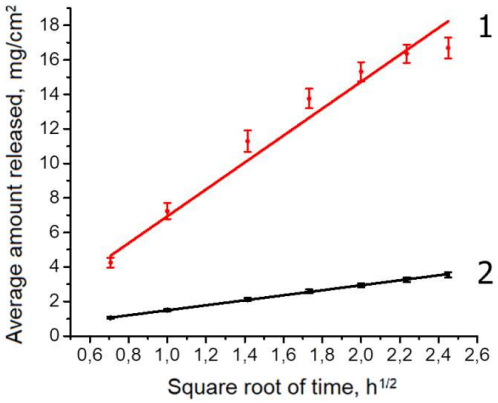

Fig. 15. Dexpanthenol release rate plots in the case of release from: 1 – 5% solution; 2 – Bepanthen® Plus cream

5. Discussion of research results

The rheological parameters of hydrophilic cream bases were contingent upon the mass ratio of M20CSE to CSA (Fig. 2). This phenomenon is due to the microstructure of compatible associates and adsorption layers of these two excipients. It is noteworthy that the maximum apparent viscosity of the o/w emulsion was approximately fourfold higher than that of the dispersion (cream base without of the oil phase).

The study of the cream bases was conducted using the spin probe method, which involved the use of four spin probes based on fatty acids. These probes were utilised to detect varying levels of the nonpolar component of associates/adsorption layers. The primary characteristics of the microstructure of mixed aggregates of nonionic surfactant and CSA were elucidated, thereby providing a foundation for understanding the formation of coagulation structures with high apparent viscosity at relatively low total concentrations of emulsifiers in dispersed systems. The formation of coagulation structures in these dispersed systems is contingent upon the following conditions:

– lateral phase distribution in aggregates/adsorption layers accompanied by the formation of solid hydrophobic CSA domains and liquid hydrophilic domains of nonionic surfactant;

– presence of solid CSA domains at the interface with the dispersion medium and ordered packing along the entire length of the alkyl chains;

– adequate hydration of mixed aggregates and adsorption layers at the interface with the dispersion medium, provided by nonionic surfactant domains;

– non-spherical configuration of mixed aggregates and adsorption layer domains.

Another condition for the formation of coagulation structures is a sufficient concentration of particles with the specified properties. A decline in the total concentration of M20CSE and CSA (3.0 : 7.0) in dispersions resulted in a decrease in rheological parameters (Fig. 16), and at a concentration of 2.0%, a Newtonian liquid was formed.

The microstructure of the associates depended on the mass ratio of the nonionic surfactant (M20CSE) to CSA (Fig. 3–9).

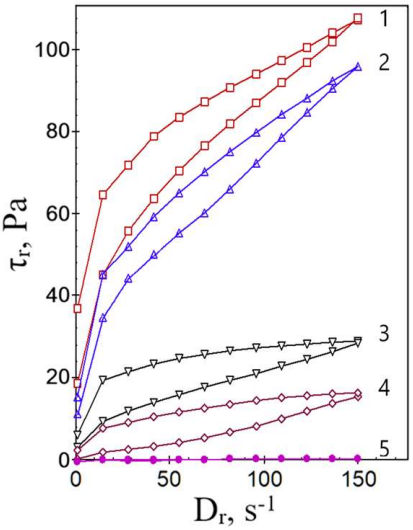

Fig. 16. Rheograms (at 25°C) of bases containing M20CSE and CSA (3.0:7.0) at their total concentration: 1 – 10%, 2 – 8%, 3 – 6%, 4 – 4%, 5 – 2%

It was demonstrated by in vitro experiments that the coagulation structure in cream bases (both without an oil phase and those containing one) was a factor that significantly reduced the release parameters of ofloxacin.

The findings of the studies were corroborated when Bepanthen® Plus cream was utilized as the test object [28, 29]. The preparation is an o/w emulsion stabilized with another nonionic surfactant, namely macrogol 40 stearate (HLB = 16.9) [30] at a concentration of 3.0%, as well as a mixture of cetyl and stearyl alcohol at concentrations of 3.6% and 2.4%, respectively. The mass ratio of nonionic surfactant to the total content of aliphatic alcohols in this cream is 3:6. (Note: According to BASF, the HLB of M20CSE is 15.0, and in the product Kolliwax CSA 50 contains cetyl and stearyl alcohols in a ratio of 5:5). Both in the case of the model emulsion and in the case of the commercially available cream, the EPR spectra of spin probes 1, 2, 3, and 4 are similar in configuration (Fig. 9, a, 14). The formation of a coagulation structure in Bepanthen® Plus cream significantly retarded the release of dexpanthenol, which is a very soluble in water [1].

Practical relevance. The results obtained provide a theoretical basis for the development of cream formulations using surfactants and CSA.

Study limitations. This paper presents the findings of studies conducted on cream bases containing CSA only with non-ionic surfactant.

Prospects for further research include studying similar cream bases with different surfactants, such as anionic or cationic ones. Furthermore, subsequent research may be focused on the release of various kinds of active substances from the cream bases.

6. Conclusions

The rheological characteristics of hydrophilic cream bases are contingent on the microstructure of mixed aggregates or adsorption layers formed by nonionic surfactant and CSA. These properties can be modified by adjusting the mass ratios between these emulsifiers. In the case of cream bases, where a coagulation structure has formed, the release of active ingredients is found to be significantly retarded.

Conflict of interests

The authors confirm that they have no conflict of interest related to this research, whether financial, personal, authorship or otherwise, that could affect the research and its results presented in this article.

Funding

The research was financially supported by the National Academy of Sciences of Ukraine within the framework of the project «Study of dispersed systems with liquid dispersion medium as the primary matrices for medicinal products» (0125U000740).

Data availability

Data will be made available on reasonable request.

Use of artificial intelligence

The authors confirm they did not use artificial intelligence technologies when creating the current work.

Author Contributions

Nikolay Lyapunov and **Olena Bezugla:** Conceptualization, Methodology, Writing, Supervision; **Anna Liapunova:** Investigation (*in vitro* release test), Visualization; **Igor Zinchenko:** Investigation (liquid chromatography), Visualization; **Oleksii Liapunov:** Investigation (EPR spectroscopy), Visualization; **Yurij Stolper:** Investigation (rotational viscometry). All authors have revised and approved the manuscript.

References

1. The European Pharmacopoeia (2022). European Directorate for the Quality of Medicines & HealthCare of the Council of Europe. Strasbourg: Council of Europe, 6106. Available at: http://pheur.edqm.eu/subhome/11-8

2. Derzhavna Farmakopeia Ukrainy. Vol. 2 (2024). Kharkiv: Derzhavne pidpryiemstvo «Ukrainskyi naukovyi farmakopeinyi tsentr yakosti likarskykh zasobiv», 424.

3. Costa, C., Medronho, B., Filipe, A., Mira, I., Lindman, B., Edlund, H., Norgren, M. (2019). Emulsion Formation and Stabilization by Biomolecules: The Leading Role of Cellulose. Polymers, 11 (10), 1570. https://doi.org/10.3390/polym11101570

4. Langevin, D. (2023). Recent Advances on Emulsion and Foam Stability. Langmuir, 39 (11), 3821–3828. https://doi.org/10.1021/acs.langmuir.2c03423

5. Lyapunova, A. M., Bezugla, O. P., Lyapunov, O. M. (2017). The study of o/w emulsions using the rotating viscometer method and the method of spin probes. News of Pharmacy, 4 (92), 29–34. https://doi.org/10.24959/nphj.17.2190

6. Dekker, R. I., Velandia, S. F., Kibbelaar, H. V. M., Morcy, A., Sadtler, V., Roques-Carmes, T. et al. (2023). Is there a difference between surfactant-stabilised and Pickering emulsions? Soft Matter, 19 (10), 1941–1951. https://doi.org/10.1039/d2sm01375d

7. Karishma, S., Rajvanshi, K., Kumar, H., Basavaraj, M. G., Mani, E. (2023). Oil-in-Water Emulsions Stabilized by Hydrophilic Homopolymers. Langmuir, 39 (38), 13430–13440. https://doi.org/10.1021/acs.langmuir.3c00798

8. Ataeian, P., Aroyan, L., Parwez, W., Tam, K. C. (2022). Emulsions undergoing phase transition: Effect of emulsifier type and concentration. Journal of Colloid and Interface Science, 617, 214–223. https://doi.org/10.1016/j.jcis.2022.02.140

9. Zheng, R., Tian, J., Binks, B. P., Cui, Z., Xia, W., Jiang, J. (2022). Oil-in-Water emulsions stabilized by alumina nanoparticles with organic electrolytes: Fate of particles. Journal of Colloid and Interface Science, 627, 749–760. https://doi.org/10.1016/j.jcis.2022.07.085

10. Badruddoza, A. Z. M., Yeoh, T., Shah, J. C., Walsh, T. (2023). Assessing and Predicting Physical Stability of Emulsion-Based Topical Semisolid Products: A Review. Journal of Pharmaceutical Sciences, 112 (7), 1772–1793. https://doi.org/10.1016/j.xphs.2023.03.014

11. Binks, B. P. (Ed.) (1998). Modern aspects of Emulsion Science. Royal Society of Chemistry, 442. https://doi.org/10.1039/9781847551474

12. Myers, D. (2006). Surfactant Science and Technology. John Wiley & Sons, Inc. https://doi.org/10.1002/047174607X

13. Farn, R. J. (Ed.) (2006). Chemistry and Technology of Surfactants. Blackwell Publishing Ltd, 315. https://doi.org/10.1002/9780470988596

14. Cai, Z., Wei, Y., Shi, A., Zhong, J., Rao, P., Wang, Q., Zhang, H. (2023). Correlation between interfacial layer properties and physical stability of food emulsions: current trends, challenges, strategies, and further perspectives. Advances in Colloid and Interface Science, 313, 102863. https://doi.org/10.1016/j.cis.2023.102863

15. Li, P., Huang, H., Fang, Y., Wang, Y., No, D. S., Bhatnagar, R. S., Abbaspourrad, A. (2023). Interfacial engineering of clear emulsions: Surfactant hydrophobicity and the hidden role of chain structure. Colloids and Surfaces A: Physicochemical and Engineering Aspects, 676, 132242. https://doi.org/10.1016/j.colsurfa.2023.132242

16. Botti, T. C., Hutin, A., Quintella, E., Carvalho, M. S. (2022). Effect of interfacial rheology on drop coalescence in water–oil emulsion. Soft Matter, 18(7), 1423–1434. https://doi.org/10.1039/d1sm01382c

17. Leister, N., Götz, V., Jan Bachmann, S., Nachtigall, S., Hosseinpour, S., Peukert, W., Karbstein, H. (2023). A comprehensive methodology to study double emulsion stability. Journal of Colloid and Interface Science, 630, 534–548. https://doi.org/10.1016/j.jcis.2022.10.119

18. Han, D., Mao, J., Zhao, J., Zhang, H., Wang, D., Cao, H. et al. (2022). Dissipative particle dynamics simulation and experimental analysis of effects of Gemini surfactants with different spacer lengths on stability of emulsion systems. Colloids and Surfaces A: Physicochemical and Engineering Aspects, 655, 130205. https://doi.org/10.1016/j.colsurfa.2022.130205

19. McClements, D. J., Jafari, S. M. (2018). Improving emulsion formation, stability and performance using mixed emulsifiers: A review. Advances in Colloid and Interface Science, 251, 55–79. https://doi.org/10.1016/j.cis.2017.12.001

20. Hong, I. K., Kim, S. I., Lee, S. B. (2018). Effects of HLB value on oil-in-water emulsions: Droplet size, rheological behavior, zeta-potential, and creaming index. Journal of Industrial and Engineering Chemistry, 67, 123–131. https://doi.org/10.1016/j.jiec.2018.06.022

21. Alam, S., Algahtani, M. S., Ahmad, M. Z., Ahmad, J. (2020). Investigation Utilizing the HLB Concept for the Development of Moisturizing Cream and Lotion: In-Vitro Characterization and Stability Evaluation. Cosmetics, 7 (2), 43. https://doi.org/10.3390/cosmetics7020043

22. Wang, Q., Zhang, H., Han, Y., Cui, Y., Han, X. (2023). Study on the relationships between the oil HLB value and emulsion stabilization. RSC Advances, 13 (35), 24692–24698. https://doi.org/10.1039/d3ra04592g

23. Colafemmina, G., Palazzo, G., Mateos, H., Amin, S., Fameau, A.-L., Olsson, U., Gentile, L. (2020). The cooling process effect on the bilayer phase state of the CTAC/cetearyl alcohol/water surfactant gel. Colloids and Surfaces A: Physicochemical and Engineering Aspects, 597, 124821. https://doi.org/10.1016/j.colsurfa.2020.124821

24. Tran, H. H., Nguyen, T. H., Tran, T. T., Vu, H. D., Nguyen, H. M. T. (2021). Structures, Electronic Properties, and Interactions of Cetyl Alcohol with Cetomacrogol and Water: Insights from Quantum Chemical Calculations and Experimental Investigations. ACS Omega, 6 (32), 20975–20983. https://doi.org/10.1021/acsomega.1c02439

25. Berliner, L. J., Reuben, J. (Ed.) (1989). Spin Labeling: Theory and Applications. New York: Plenum Press, 670. https://doi.org/10.1007/978-1-4613-0743-3

26. Bezuglaya, E., Lyapunov, N., Chebanov, V., Liapunov, O. (2022). Study of the formation of micelles and their structure by the spin probe method. ScienceRise: Pharmaceutical Science, 4 (38), 4–18. https://doi.org/10.15587/2519-4852.2022.263054

27. Liapunov, M. O., Ivanov, L. V., Bezugla, O. P., Zhdanov, R. I., Tsymbal, L. V. (1992). Doslidzhennia ahrehativ poverkhnevo-aktyvnykh rechovyn (PAR) metodom spinovykh zondiv. Farmatsevtychnyi zhurnal, 5-6, 40–45.

28. Buckingham, R. (Ed.) (2020). Martindale: The Complete Drug Reference, 40th Ed. London: Pharmaceutical Press, 4852.

29. Derzhavnyi reiestr likarskykh zasobiv Ukrainy. Available at: http://www.drlz.kiev.ua/

30. Sheskey, P. J., Hancock, B. C., Moss, G. P., Goldfarb, D. J. (Eds.) (2020). Handbook of Pharmaceutical Excipients. London: Pharm. Press, 1296.

31. Liapunova, A. M., Krasnopyorova, A. P., Bezugla, O. P., Liapunov, O. M., Yukhno, G. D., Pukhova, T. M. (2024). Polythermal studies of the water – propylene glycol systems by densitometry, viscometry and spin probes method. Functional Materials, 31 (4), 609–618. https://doi.org/10.15407/fm31.04.609

32. Ilić, T., Pantelić, I., Savić, S. (2021). The Implications of Regulatory Framework for Topical Semisolid Drug Products: From Critical Quality and Performance Attributes towards Establishing Bioequivalence. Pharmaceutics, 13 (5), 710. https://doi.org/10.3390/pharmaceutics13050710

33. Tiffner, K. I., Kanfer, I., Augustin, T., Raml, R., Raney, S. G., Sinner, F. (2018). A comprehensive approach to qualify and validate the essential parameters of an in vitro release test (IVRT) method for acyclovir cream, 5%. International Journal of Pharmaceutics, 535 (1-2), 217–227. https://doi.org/10.1016/j.ijpharm.2017.09.049

34. Lyapunov, N., Bezugla, O., Liapunova, A., Zinchenko, I., Liapunov, O., Lysokobylka, O., Dzhoraieva, S. (2025). Study of some properties of hydrophilic ointment bases depending on their composition. ScienceRise: Pharmaceutical Science, 5 (57), 4–19. https://doi.org/10.15587/2519-4852.2025.339597

35. Bezuglaya, E., Liapunova, A., Zinchenko, I., Lyapunov, N. (2023). Study of factors affecting the in vitro release of dexpanthenol from solutions and topical semi-solid preparations. ScienceRise: Pharmaceutical Science, 3 (43), 4–15. https://doi.org/10.15587/2519-4852.2023.279283

Received 11.03.2026
Received in revised form 07.04.2026
Accepted 21.04.2026
Published 30.04.2026

Nikolay Lyapunov, Doctor of Pharmaceutical Sciences, Professor, Leading Researcher**,** Department of Technology and Analysis of Medicinal Products**,** Institute of Functional Materials Chemistry**,** State Scientific Institution «Institute for Single Crystals» of National Academy of Sciences of Ukraine**,** Nauky ave., 60, Kharkiv, Ukraine, 61072
ORCID: https://orcid.org/0000-0002-5036-8255

O**lena Bezugla***, PhD, Senior Researcher, Head of Department, Department of Technology and Analysis of Medicinal Products, Institute of Functional Materials Chemistry, State Scientific Institution «Institute for Single Crystals» of National Academy of Sciences of Ukraine, Nauky ave., 60, Kharkiv, Ukraine, 61072
ORCID: https://orcid.org/0000-0002-3629-7059

Oleksii Liapunov, PhD, Researcher, Department of Technology and Analysis of Medicinal Products, Institute of Functional Materials Chemistry, State Scientific Institution «Institute for Single Crystals» of National Academy of Sciences of Ukraine, Nauky ave., 60, Kharkiv, Ukraine, 61072
ORCID: https://orcid.org/0000-0001-6103-7489

Anna Liapunova, PhD, Senior Researcher, Deputy Head of Department, Department of Technology and Analysis of Medicinal Products, Institute of Functional Materials Chemistry, State Scientific Institution «Institute for Single Crystals» of National Academy of Sciences of Ukraine, Nauky ave., 60, Kharkiv, Ukraine, 61072
ORCID: https://orcid.org/0000-0001-7997-3929

Igor Zinchenko, PhD, Senior Researcher, Department of Technology and Analysis of Medicinal Products, Institute of Functional Materials Chemistry, State Scientific Institution «Institute for Single Crystals» of National Academy of Sciences of Ukraine, Nauky ave., 60, Kharkiv, Ukraine, 61072
ORCID: https://orcid.org/0000-0003-0562-689X

Yurij Stolper, PhD, Senior Researcher**,** Department of Technology and Analysis of Medicinal Products**,** Institute of Functional Materials Chemistry**,** State Scientific Institution «Institute for Single Crystals» of National Academy of Sciences of Ukraine
Nauky ave., 60, Kharkiv, Ukraine, 61072
ORCID: https://orcid.org/0000-0001-7652-7624

***Corresponding author:** *Olena Bezugla, e-mail: bezugla.op@gmail.com*